



저작자표시-비영리-변경금지 2.0 대한민국

이용자는 아래의 조건을 따르는 경우에 한하여 자유롭게

- 이 저작물을 복제, 배포, 전송, 전시, 공연 및 방송할 수 있습니다.

다음과 같은 조건을 따라야 합니다:



저작자표시. 귀하는 원저작자를 표시하여야 합니다.



비영리. 귀하는 이 저작물을 영리 목적으로 이용할 수 없습니다.



변경금지. 귀하는 이 저작물을 개작, 변형 또는 가공할 수 없습니다.

- 귀하는, 이 저작물의 재이용이나 배포의 경우, 이 저작물에 적용된 이용허락조건을 명확하게 나타내어야 합니다.
- 저작권자로부터 별도의 허가를 받으면 이러한 조건들은 적용되지 않습니다.

저작권법에 따른 이용자의 권리는 위의 내용에 의하여 영향을 받지 않습니다.

이것은 [이용허락규약\(Legal Code\)](#)을 이해하기 쉽게 요약한 것입니다.

[Disclaimer](#)

공학석사학위논문

**An Experimental Study on
Ignition Delay Characteristics of
Isooctane-Ethanol Blend Fuel for Knocking
Prevention in Spark Ignition Engine**

불꽃점화 엔진에서 노킹 방지를 위한
이소옥탄-에탄올 혼합 연료의
점화지연 특성에 관한 실험적 연구

2013년 2월

서울대학교 대학원

기계항공공학부

송 화 섭

An Experimental Study on Ignition Delay Characteristics of Isooctane-Ethanol Blend Fuel for Knocking Prevention in Spark Ignition Engine

지도교수 송 한 호

이 논문을 공학석사 학위논문으로 제출함

2012 년 12 월

서울대학교 대학원

기계항공공학부

송 화 섭

송화섭의 공학석사 학위논문을 인준함

2013 년 2 월

위원장 김 찬 중

부위원장 송 한 호

위 원 김 민 수



Abstract

An Experimental Study on
Ignition Delay Characteristics of
Isooctane–Ethanol Blend Fuel for
Knocking Prevention in Spark Ignition
Engine

Hwasup Song

School of Mechanical and Aerospace Engineering

The Graduate School

Seoul National University

Downsizing and greenhouse gas reduction are the primary interests of automotive industry for the 21st century. These trends face with technically challenging problems, and “knock” or “knocking” is one of them. In relation to knock phenomenon study, ignition delays of isooctane–ethanol blend fuel under various conditions are measured by using a rapid compression machine and experimental results are analyzed

by chemical kinetics. Results show that ignition delay tends to be considerably longer with the addition of ethanol into isooctane under 800 - 840 K region, but this characteristic of ethanol as a reaction-delaying agent diminishes as various blends show similar reactivity under 850 - 880 K region. In addition to that, there is no significant difference of test results when ethanol content in blended fuel is more than 50 %. Analyses on these cases show that different reaction pathway of ethanol under the test conditions is a key in understanding experimental results, nevertheless additional work to the kinetic models would fairly improve the accuracy of computational studies to a certain extent.

Keywords: ignition delay, knock, rapid compression machine, chemical kinetics, isooctane-ethanol blend

Student Number: 2011-20716

Abstract	_____	i
Contents	_____	iii
List of Tables	_____	iv
List of Figures	_____	v
1. Introduction	_____	1
1.1 Downsizing and Greenhouse Gas Reduction	_____	1
1.2 Engine Knock	_____	3
1.3 Octane Number	_____	4
1.4 Objectives	_____	6
2. Modeling Descriptions	_____	10
2.1 Two-zone Model of Spark-Ignition Engine	_____	10
2.2 Ignition Delay	_____	13
2.3 Chemical Kinetics Mechanism	_____	15
3. Experimental Setup	_____	17
3.1 Rapid Compression Machine	_____	17
3.2 Pressure Data Processing	_____	20
4. Results and Discussion	_____	28
4.1 Experimental Results	_____	28
4.2 Chemical Kinetics Modeling Analysis	_____	30
4.3 Limitations and Future Works	_____	35
5. Conclusions	_____	47
References	_____	49
Abstract (in Korean)	_____	52

List of Tables

Table 1.1 Test conditions for octane number measurement

Table 2.1 Maximum temperature and pressure of the unburned zone

Table 3.1 Specifications of RCM

List of Figures

Figure 3.1 Schematic of RCM

Figure 3.2 Operating scheme of RCM

Figure 3.3 Hydraulic circuit diagram of RCM

Figure 3.4 Typical pressure profile of an RCM experiment

Figure 4.1 Measured ignition delays of blends

Figure 4.2 Reaction rates of $i\text{-C}_8\text{H}_{18} + \text{H} \rightarrow \text{R} + \text{H}_2$

Figure 4.3 Alkyl radical mass versus time at 800 K, E0

Figure 4.4 Alkyl radical mass versus time at 800 K, E10

Figure 4.5 Alkyl radical mass versus time at 800 K, E20

Figure 4.6 Alkyl radical mass versus time at 800 K, E50

Figure 4.7 RO_2 radical mass versus time at 800 K, E0

Figure 4.8 RO_2 radical mass versus time at 800 K, E10

Figure 4.9 RO_2 radical mass versus time at 800 K, E20

Figure 4.10 RO_2 radical mass versus time at 800 K, E50

Figure 4.11 Reaction rates of $\text{C}_2\text{H}_5\text{OH} (+ \text{M}) \rightarrow \text{CH}_2\text{OH} + \text{CH}_3 (+ \text{M})$

Figure 4.12 Magnification of Figure 4.11

Figure 4.13 Alkyl radical mass versus time at 860 K, E0

Figure 4.14 Alkyl radical mass versus time at 860 K, E10

Figure 4.15 Alkyl radical mass versus time at 860 K, E20

Figure 4.16 Alkyl radical mass versus time at 860 K, E50

Figure 4.17 Reaction rates of (23)

Figure 4.18 Comparison of experimental and computational results

1. Introduction

1.1 Downsizing and Greenhouse Gas Reduction

Today's trend of the automotive industry is mainly focused on manufacturing "more efficient" and "less polluting" vehicles. In general, power output of an engine is proportional to its displacement volume, therefore today's smaller engines are often misunderstood to have less maximum work output than large ones of the past generation. This is true if the small one is operated under naturally aspirated condition. Turbochargers are usually supplemented for boosting intake pressure to compensate for the power deficiency. The word 'downsizing' comes out from this trend of applying smaller engine to the vehicle. In order to compare the pure working ability of an engine, we need to normalize the power by cancelling out the volumetric merit, in detail dividing the power output of an engine by its own displacement volume. In this way the unit of a normalized power becomes same as that of a pressure, called "mean effective pressure (MEP)." Turbocharged engines tend to have higher MEP than naturally aspirated case as both pressure and temperature of the former are higher than the latter for providing enough power from limited engine size. Benefit of downsizing mostly comes from the fact that smaller displacement volume leads to decreased tail-pipe emissions.

Downsized engines are also lightened in weight due to less materials needed, thereby fuel consumption of a vehicle is additionally improved.

Another way of greenhouse gas reduction is utilizing cleaner fuel, for example, substituting biofuel for traditional fossil fuel. Biofuels come from various feedstock such as corn, sugar cane, biomass, algae, etc. Usually the raw materials pass through fermentation process and additional synthesis or chemical, biological processes are needed for conversion to bioethanol, biodiesel, bio ethers or biogas. Currently, bioethanol is the main type of the kind and it is mixed to a certain extent with traditional gasoline and sold to public in some countries. For example, Brazil has been managing a ethanol fuel program for almost 40 years which mandates the blending of ethanol with gasoline, so that pure gasoline is no longer available on market in the country [1]. When ethanol is mixed with gasoline, the fuel is indicated e.g., E10, which stands for 10 % ethanol plus 90 % gasoline in volume fraction. U.S. government and state of California has also been enacting legislations for mandating the use of clean fuel in transportation sector. These programs like low-carbon fuel standard (LCFS) or renewable fuels standard extended (RFS2) have given rise to the interest to utilization of gasoline-ethanol blend throughout the nation.

1.2 Engine Knock

High MEP conditions operated by downsizing is responsible for severe operating condition of an engine which may cause abnormal combustion phenomena. In case of a 4-stroke spark ignition (SI) engine, fuel-air mixture is inducted into the cylinder during the intake process and compressed, followed by ignition from an ignition source (i.e., a spark plug) and combustion. Throughout the combustion process, inside of the cylinder can be divided into two zones - the burned zone and the unburned zone. Normally fuel-air mixture is ignited by a spark plug when the piston is travelling upward, slightly ahead of top dead center (TDC) position. Then the flame kernel is formed and it consumes surrounding unburned gas at the flame front, followed by flame propagation to the unburned gas region. At the flame surface chemical reaction between fuel and air occurs and after the flame has passed over, the temperature and pressure of the burned gas region is elevated. Burn duration of the fuel-air mixture remains within a definite period of time, usually an order of a millisecond. Temperature and pressure of the unburned zone gradually increases during the burn duration, mainly due to the radiative heat transfer from the hot burned gas just prior to the reach of the flame, along with compressive heating by the piston's upward motion which accounts for additive amount of temperature and pressure increase.

Now the end gas, the very last part of the mixture remaining at the unburned zone, is under considerable pressure and temperature conditions. If conditions are sufficient to self-ignite the end gas, irregular combustion occurs before the flame reaches and undesirable pressure pulse is formed, which may cause material damage of the piston or the cylinder wall. When this pressure pulse hits the cylinder wall audible noise occurs and this phenomenon is called knock or knocking.

1.3 Octane Number

Knock may cause reduced performance and serious material damage to an SI engine. Therefore, the need for an index of comparing knock characteristics of fuels used in SI engines arises. Fuels have different chemical and physical properties. For an SI engine, gasoline is used as a primary fuel, but since gasoline itself is a chemical compound of hundreds of elements and its own properties, quality, and additives vary with petroleum refining company, the self-ignition characteristics of gasoline from different brand cannot be identical.

Octane number (ON) is the index by which anti-knock behavior of the fuel is represented. ON determination procedure of a given fuel is as follows:

1. Fuel is tested in a certain test equipment called cooperative fuel research (CFR) engine under specific operating conditions, in detail knock is induced via intentionally severe engine operation (e.g., increased compression ratio.)
2. When knock occurs, blend of isooctane ($i\text{-C}_8\text{H}_{18}$, 2,2,4-trimethylpentane) and normal heptane ($n\text{-C}_7\text{H}_{16}$) is now tested under the same conditions. Two respective chemicals are selected because they have contrastive reactivity that knock propensity of n-heptane is stronger while isooctane is not.
3. If pure isooctane is tested in CFR engine and exhibits same knock phenomenon as that of test fuel under same test conditions, its ON is given as 100. If pure n-heptane is used then ON of test fuel is 0. Blend of isooctane and n-heptane shows knock resistance between ON of 100 and 0. In case of a certain test fuel which has same knock characteristics to the blend of 90% isooctane and 10% n-heptane, then the fuel is given ON of 90.

There are two different ways of ON measurement, research octane number (RON) and motor octane number (MON). MON is acquired under relatively severe test conditions than RON test. Mean value of RON and MON is widely adopted as ON. Detailed test conditions are given in Table 1.1 [2]. In either case whether we focus on RON or MON, It is

clear that higher ON fuel assures stronger anti-knock behavior. Normal unleaded gasoline fuels have an ON ranging from 87 to 95 worldwide while premium gasoline fuels tend to have almost 98 to 100. In some cases fuel may resist knock to the further extent than pure isooctane, then ON is measured in this way; tetraethyl lead (TEL) which is known as a good anti-knock agent is added to pure isooctane. Volume fraction of additive TEL is summed up over 100. For example, ethanol has RON of 108.

1.4 Objectives

Gasoline-ethanol blend fuel has been widely used for quite a long time, but there are few studies on characteristics of blends, either in chemical kinetics modeling or in experimental research. Cancino et al [3] measured self-ignition characteristics of ethanol-containing multi-component fuel in a shock tube and studied chemical kinetics of corresponding reactions. Dagaut and Togbé [4] carried out an experimental study on oxidation kinetics of isooctane-ethanol mixture in a jet-stirred reactor. Kasseris and Heywood [5, 6] presented the new concept of ON, as they proposed the “effective ON” of ethanol-gasoline blends in SI, direct injection engine which also accounts for the additional anti-knock behavior of ethanol from its massive evaporative charge cooling effect.

Gasoline is a compound of hundreds of chemical substances such as hydrocarbons containing up to 12 carbon atoms per molecule. These include paraffins, olefins, naphthenes, and small amount of aromatics, but their mixing ratio depends on the refineries since they don't have same process for production and type of crude oil feed. On account of these facts, gasoline is not suitable for use in chemical kinetics modeling or analysis. Substances of commercial gasoline are complex and not fully examined and reaction pathways of many substances are still unknown, which gives only limited approach. In fact, "pure" chemicals are often used as a surrogate of gasoline in combustion studies, especially when investigation of chemical kinetics is a major objective. Isooctane, which is the basic surrogate fuel of gasoline, is selected in this study.

From literature survey above, we recognize that interest on gasoline-ethanol blend has been raised recently but fundamental combustion studies are not performed in depth. Hence objectives of this study are as follows:

- 1) identification of ignition characteristics of the isooctane-ethanol blend fuel
- 2) understanding of chemical reaction kinetics of the blend

Approaches to this study include both computational and experimental

studies. In chapter 2, engine knock conditions are investigated with computational approach which simulate the in-cylinder situations during compression and combustion processes. Two-zone model for an SI engine and the definition of ignition delay are described and explanation of chemical kinetic mechanisms applied in this study is also given. Conditions for experimental study are set with the calculated knock conditions. In chapter 3, operating fundamentals and design considerations of a rapid compression machine for ignition delay measurement are described. Finally, in chapter 4 experimental results are given and analyses of test results are performed using chemical kinetics model. Limitations and future works of this study are also mentioned. Research grade isooctane (Aldrich, >99.9%) is used as a surrogate of gasoline and blended with anhydrous ethanol (Aldrich, 99.5%).

	RON	MON
Engine Speed (RPM)	600	900
Inlet Air Temp. (°C)	52	149
Coolant Temp. (°C)	100	100
Oil Temp. (°C)	57	57
Ignition Timing	13° bTDC	19° - 26° bTDC
Spark Plug Gap (mm)	0.508	0.508
Inlet Air Pressure	atmospheric pressure	
Air/Fuel Ratio	adjusted for maximum knock	
Compression Ratio	adjusted to get standard knock	

Table 1.1 Test conditions for octane number measurement

2. Modeling Descriptions

2.1 Two-zone Model of Spark-Ignition Engine

For the purpose of investigating the relationship between knock occurrence and combustion characteristics of isooctane-ethanol blend under SI engine operating conditions, two-zone SI engine model is studied for mapping the temperature and pressure range of the unburned zone in SI engine. For thermodynamic modeling and calculation Cantera Toolbox combined with MATLAB R2011b version is used.

Inside of the cylinder is considered to be composed of two independent zones - the unburned zone and the burned zone. Flame consumes the fuel-air mixture and propagates so that the volume of the unburned zone continuously decreases while burned zone expands. Their respective volume, mass, and enthalpy also vary throughout the flame propagating process while pressure of each zone is thought to be identical at every moment. With these properties it is possible to obtain pressure-time and temperature-time profiles of each zone by using energy equations [7]

$$0 = \dot{M}_v h_u + \dot{Q}_u + P_c \frac{dV_u}{dt} + \frac{dU_u}{dt}$$

for the unburned zone and

$$\dot{M}_b h_u = \dot{Q}_b + P_c \frac{dV_b}{dt} + \frac{dU_b}{dt}$$

for the burned zone.

Mass equations of respective zones are

$$0 = \dot{M}_b - \frac{dM_u}{dt}$$

and

$$\dot{M}_u = \frac{dM_b}{dt}$$

Total volume inside the cylinder can be expressed as

$$V_c = V_u + V_b = \frac{M_u R_u T_u}{P_c} + \frac{M_b R_b T_b}{P_c}$$

Multiplying by P_c and then differentiating, above expression becomes

$$V_c \frac{dP_c}{dt} + P_c \frac{dV_c}{dt} = M_u \dot{\alpha}_u \frac{dT_u}{dt} + M_b \dot{\alpha}_b \frac{dT_b}{dt} + \dot{M}_b (\alpha_b - \alpha_u)$$

where $\alpha(T) = RT$ and $\dot{\alpha} = \frac{d\alpha}{dt}$.

By substituting $H = U + PV$ into energy equations, we can rewrite them as

$$0 = \dot{M}_b h_u + \dot{Q}_u - V_u \frac{dP_c}{dt} + \frac{dH_u}{dt}$$

and

$$\dot{M}_b h_u = \dot{Q}_b - V_b \frac{dP_c}{dt} + \frac{dH_b}{dt}$$

By adopting an ideal gas law, $dh = C_p dT$ can be applied to the expressions and thus energy equations become

$$M_u C_{p,u} \frac{dT_u}{dt} = V_u \frac{dP_c}{dt} - \dot{Q}_u$$

and

$$M_b C_{p,b} \frac{dT_b}{dt} = V_b \frac{dP_c}{dt} - \dot{Q}_b + \dot{M}_b (h_u - h_b)$$

Finally, the pressure derivative $\frac{dP_c}{dt}$ can be expressed as

$$(V_c - \beta_u V_u - \beta_b V_b) \frac{dP_c}{dt} = -P_c \frac{dV_c}{dt} + \beta_b \dot{M}_b (h_u - h_b) - (\beta_u \dot{Q}_u + \beta_b \dot{Q}_b) + \dot{M}_b (\alpha_b - \alpha_u)$$

where $\beta(T) = \frac{\dot{\alpha}}{C_p}$.

Hence pressure, enthalpy, mass, and temperature of respective zones are computed and updated through the given time duration. Also the volume of each zone are acquired. In this computation process, the burn rate \dot{M}_b must be set to a specific value and this is in form

$$\dot{M}_b = A_f \rho_u V_f$$

where A_f is the projected area of the flame front to the piston surface, ρ_u is the density of the unburned gas approaching the flame front, and V_f is the velocity of the flame front relative to the unburned zone. Thus, V_f is given by

$$V_f = V_L + C_f V_{t,u}$$

where the subscripts L and t,u each stand for laminar and turbulent, respectively. C_f is a specified turbulence coefficient, approximately unity. Therefore, turbulent flame speed should be calculated first but since it

might fairly vary upon flow inside the cylinder, values by Pulkrabek [8] are adopted. Hence computed pressure–time and temperature–time profile might be different in detailed numbers if other turbulence properties are applied.

The maximum pressure and temperature of the end gas region vary by spark timing and ethanol content percentage. Here spark timing is set between 20 CAD bTDC (before Top Dead Center) - 0 CAD bTDC. This range is the typical operating limit of an SI engine. As spark timing is advanced i.e., combustion starts far ahead of end of compression, it is a natural result that the maximum temperature of the unburned gas would become higher since more heat transfer from the burned zone mainly accounts for the increase in pressure of the unburned zone. Ethanol content in fuel alters thermodynamic properties e.g., specific heat ratio, total moles of fuel–air mixture, etc., which may also cause differences in the maximum pressure and temperature. Approximate values are given in Table 2.1.

2.2 Ignition Delay

When a test gas is put into specific temperature and pressure conditions, reactions between molecules of the fuel–air mixture are stimulated. There

are different pathways that molecules are able to go through and most of these reactions are collision of molecules inside. After a moment radicals, which are very unstable species coming out from collision, are formed in large quantity and they induce consecutive reaction. Whole process of these chained reactions is called combustion when it is observed in “global” point of view.

As it is mentioned in above paragraph, it takes a moment for the massive formation of combustion radicals nevertheless the test gas is put into high temperature and pressure conditions which provides enough energy for the reactions. Duration for the massive radical formation may vary with such conditions as type of fuel, temperature, concentration, equivalence ratio, blending percentage, etc. This duration is called “ignition delay” and this is often acknowledged as a factor of reactivity of a tested mixture.

Ignition delay and anti-knock behavior have a close connection in each other. Longer ignition delay of a fuel-air mixture is directly related to the excellence in anti-knock behavior, as knock would not occur when the end gas stands against self-ignition until the flame propagates and consumes the end gas. Compared to this, fuels with short ignition delay would suffer frequent knock because of lack of endurance on self-ignition.

2.3 Chemical Kinetics Mechanism

A comprehensive chemical kinetic mechanism is adopted for computation of reactions of fuel-air mixture and calculation of ignition delay. Full isooctane mechanism developed by a research group from Lawrence Livermore National Laboratory [9] is mainly used in this study. The isooctane mechanism contains 874 species and 6,864 elementary reactions and is the developed version of well-known successful mechanism of Curran et al. [10, 11]. Nevertheless, there are only few of ethanol-related reactions included, which is thought to be a primary cause of less accuracy in reproducing the experimental results of ethanol-containing blends. Supplementary kinetics study for the ethanol case was performed using the modified ethanol mechanism [12] by Princeton University. This mechanism is consisted of 39 species and 238 elementary reactions.

	$T_{u,max}$ (K)	P_{max} (bar)
E0	745 - 932	30 - 55
E10	734 - 930	29 - 55
E20	722 - 927	27 - 54
E50	637 - 910	24 - 52
E85	628 - 866	23 - 50
E100	620 - 856	23 - 49

Table 2.1 Maximum temperature and pressure of the unburned zone

3. Experimental Setup

3.1 Rapid Compression Machine

A rapid compression machine (RCM) is utilized to measure the ignition delay of various blends. Test is performed by inducting fuel-air mixture into the combustion chamber and compressing the gas instantaneously. It tends to have the compressing time around 15 - 30 ms which is equivalent to 1000 - 2000 RPM in a real engine time scale. If it is possible to maintain compressing time to this extent, test gas in the combustion chamber experiences sudden change of thermodynamic state which makes it feasible to assume that the initial condition of the experiment is identical with that of post-compression as heat transfer to the surroundings can be neglected. This assumption is also possible in that chemical reactions during compression stroke almost does not take place, thus no significant changes to the reactivity of test gas are assumed.

Test facility consists of RCM itself, mixing chamber for preparing fuel-air mixture, hot oil circulation system for preheating the combustion chamber, and data acquisition unit. Schematic of RCM is shown in Fig. 3.1. RCM is driven by hydraulic power which ensures fast acting and withstands high post-combustion pressure inside the combustion chamber, therefore

this setup is adequate for testing real-engine situations of relative high pressure region. Further specifications are described in Table 3.1.

3.1.1 Operating procedure

An accumulator located at the rear side of a hydraulic cylinder contains pressurized oil (over 50 kgf/cm²) which is provided from a hydraulic pump driven by an electric motor. The oil pressure from this accumulator pushes a hydraulic piston when control valve is opened and this piston is located at the end position of compression stroke in a normal state. The piston is driven back by supplying pressurized oil through the outlet port of the hydraulic cylinder which has higher pressure than that on the accumulator side. After the piston is fully backed, inside of the combustion chamber is evacuated to less than 0.001 bar (absolute) and fuel-air mixture is injected and preheated for a fixed time. Preheating time is decided by the test results in which max. 3-minute term is needed for fully heated mixture. Hydraulic piston instantly moves forward by unlocking the valve which holds the hydraulic oil at the outlet port. Sudden open of the valve gives force unbalance and pressurized oil inside the accumulator drives piston forward in relatively short period. The piston inside the combustion chamber is directly connected to the hydraulic piston therefore fast compression of the test gas is guided. Operation scheme of RCM is shown in Fig. 3.2.

3.1.2 Design considerations [13]

During the compression process, the oil pressure of the accumulator drops due to expansion. Therefore the capacity of an accumulator is selected so that the oil pressure does not drop for more than 5 % of initial pressure because the back pressure of the hydraulic piston after combustion should not overcome the oil pressure from the accumulator. Diameter of the hydraulic piston is also designed considering the force balance of the same reason above. Hydraulic oil flow rate at the outlet port should be over 1,100 L/min for fast motion, thus the pipe diameter of an outlet port is selected to fulfill the flow rate. The hydraulic circuit diagram is shown in Fig. 3.3. All operations are conducted using solenoid valves, especially in case of large size valves time needed for complete opening takes more than 100 ms which is not suitable for fast acting. Therefore additional hydraulic cylinder and a small capacity accumulator are used for fast operation of an outlet port valve within 10 ms.

3.1.3 Additional instruments

For mixture preparation, a mixing chamber equipped with an electric heater and a stirring fan was used. Before preparation chamber was preheated and controlled to stay within 60 ± 2 °C range, followed by evacuation to maximum vacuum level of 0.01 bar (absolute) which ensures satisfactory vaporization of the fuel blends tested. After

evacuation blend was first injected into the mixing chamber by a laboratory grade syringe, followed by nitrogen and oxygen injection by precise control of solenoid valves. For all cases of mixture preparation, maximum amount of injected blend was restricted to stay below its corresponding vapor pressure to ensure perfect evaporation immediately after injection. Quantity of each component was decided by partial pressure measurement with an WIKA A-10 absolute pressure sensor which has resolution of 0.001 bar and non-linearity of 0.25%. Equivalence ratio of blend and air was set to 1.0 since SI engine is always operated under this condition.

Hot oil circulation unit was also designed to preheat the combustion chamber before each experiment. Preheated temperature of the cylinder is directly related to the temperature after compression; thereby testing of a blend under broad temperature domain becomes possible.

3.2 Pressure Data Processing

3.2.1 Isentropic process assumption

Pressure inside the combustion chamber during experiment can be directly acquired by means of a Kistler 6052C31 piezoelectric pressure sensor and a charge amplifier while temperature inside the chamber cannot be

measured due to hardware limitations, thus an alternative method is adopted for temperature calculation.

If compression stroke is fast enough then isentropic relationship of pressure and temperature of the test gas can be expressed as following equations

$$\int_{T_0}^{T_c} \frac{1}{\gamma-1} d \ln T = \ln (CR)$$

$$\int_{T_0}^{T_c} \frac{\gamma}{\gamma-1} d \ln T = \ln \left(\frac{P_c}{P_0} \right)$$

where γ stands for the specific heat ratio of the test gas. Other notations such as T_0, T_c, P_0, P_c represent initial temperature, adiabatically compressed temperature, initial pressure, and adiabatically compressed pressure respectively. In real situations, the specific heat ratio is a function of temperature which makes it complicated to calculate the compressed temperature. Nevertheless if the specific heat ratio is assumed to have a constant value over a narrow range of temperature, integration of these equations become rather simple, as

$$T_c = T_0 \left(\frac{P_c}{P_0} \right)^{\frac{\gamma-1}{\gamma}}$$

By adopting the concept of finite temperature range assumption and calculation, we may rewrite the equation in following format

$$T_{i+1} = T_i \left(\frac{P_{i+1}}{P_i} \right)^{\frac{\gamma(T_i) - 1}{\gamma(T_i)}}$$

Here, i-th and (i+1)-th pressure values are used to predict the (i+1)-th temperature. Hence it becomes possible to compute the consecutive temperature during the compression stroke.

3.2.2 Pressure profile

Typical case of a pressure profile acquired is shown in Fig. 3.4. Here the start of compression is decided when the recorded pressure trace steps over 110 % of an initial pressure of tested mixture. Immediately after compression has ended, the hydraulic piston slightly moves backward after collision with the small amount of remaining hydraulic oil which could not be dumped out through the outlet port. This collision causes a small fluctuation of pressure at the peak, but this can be neglected if the fluctuation intensity is limited below a certain level. For the worst case the pressure fluctuation was about 6 % of peak pressure and corresponding temperature fluctuation 3 % of peak temperature.

3.2.3 Definition of ignition delay

In this experimental study, the ignition delay of a test gas is defined as the time elapsed from the end of compression to the point where maximum pressure rise rate occurs. This is the same definition which Schreiber et al. [14] and many other researchers has used in their studies.

In addition, other definitions of an ignition delay are also available. For example, Tanaka et al. [15] defined the ignition delay as the time at which pressure rise rate reached 20 % of maximum pressure rise rate point. Therefore, calculated ignition delay of same fuel-air mixture under the identical temperature and pressure conditions may vary with different definitions.

Item	Specification
Test chamber bore (mm)	60
Stroke (mm)	90
Compression Ratio	5 - 20, depending on clearance adjustment
Compressing Time (ms)	15 - 30
Maximum Peak Pressure after Combustion (bar)	80
Maximum Peak Temperature (K)	1000
Hydraulic Accumulator Pressure (kgf/cm ²)	50 - 160

Table 3.1 Specifications of RCM

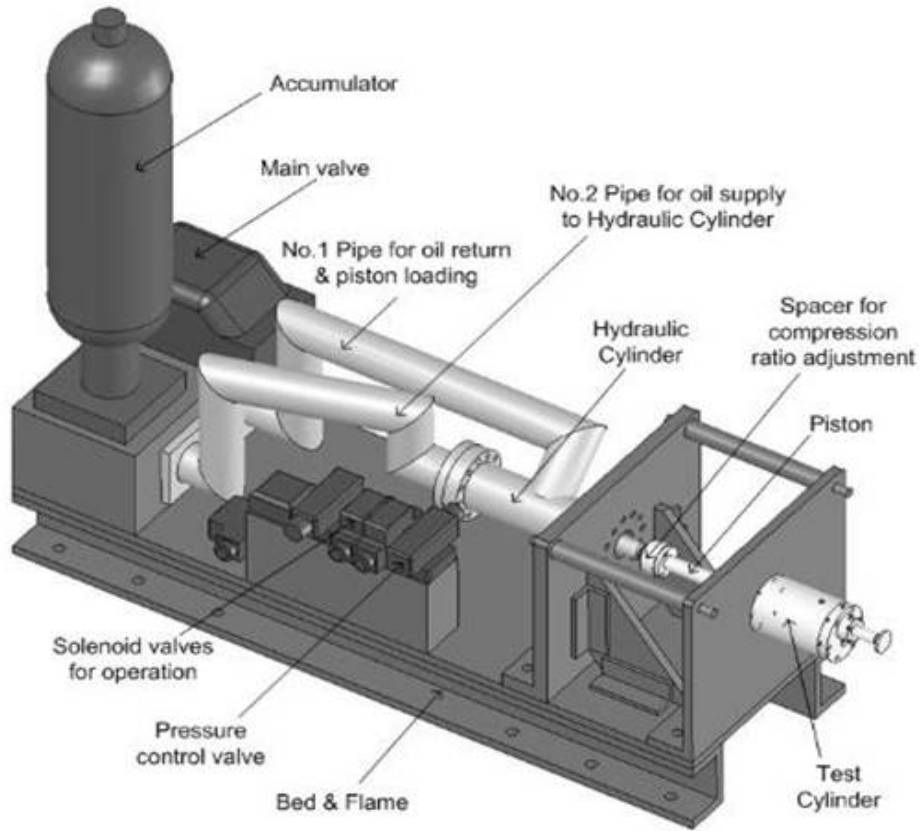


Fig. 3.1 Schematic of RCM

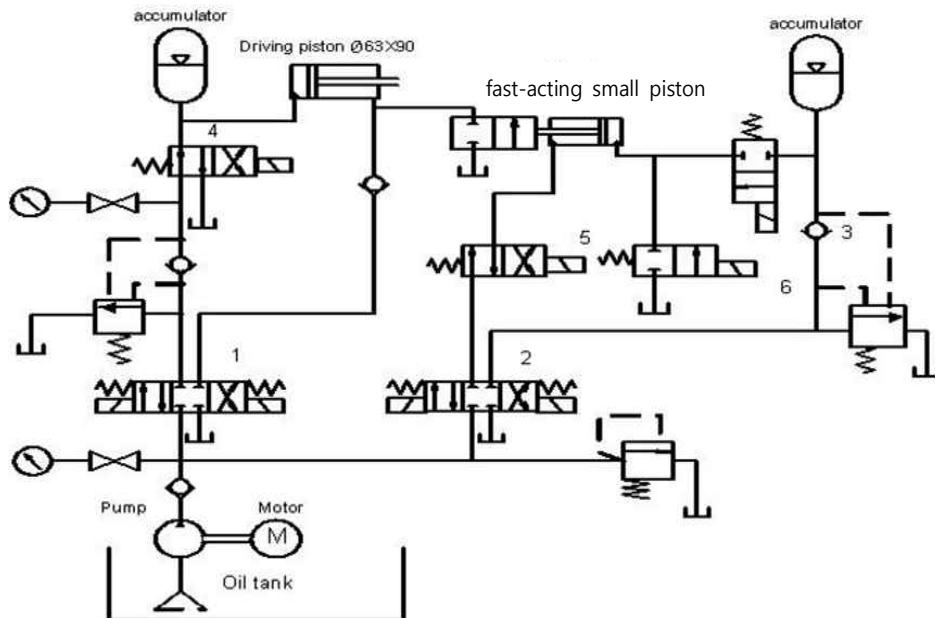


Fig. 3.3 Hydraulic circuit diagram of RCM

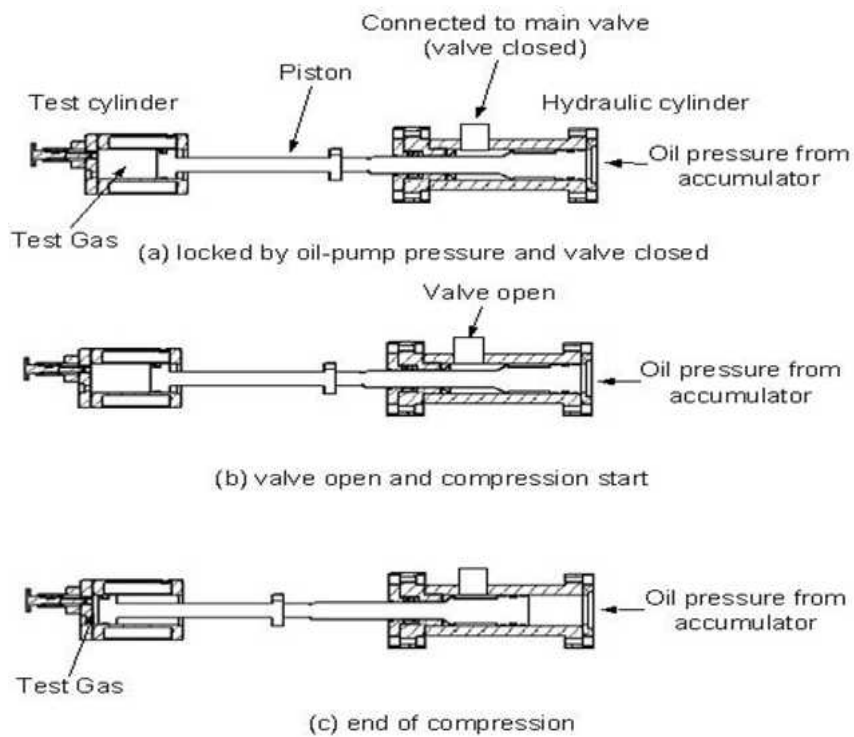


Fig 3.2 Operating scheme of RCM

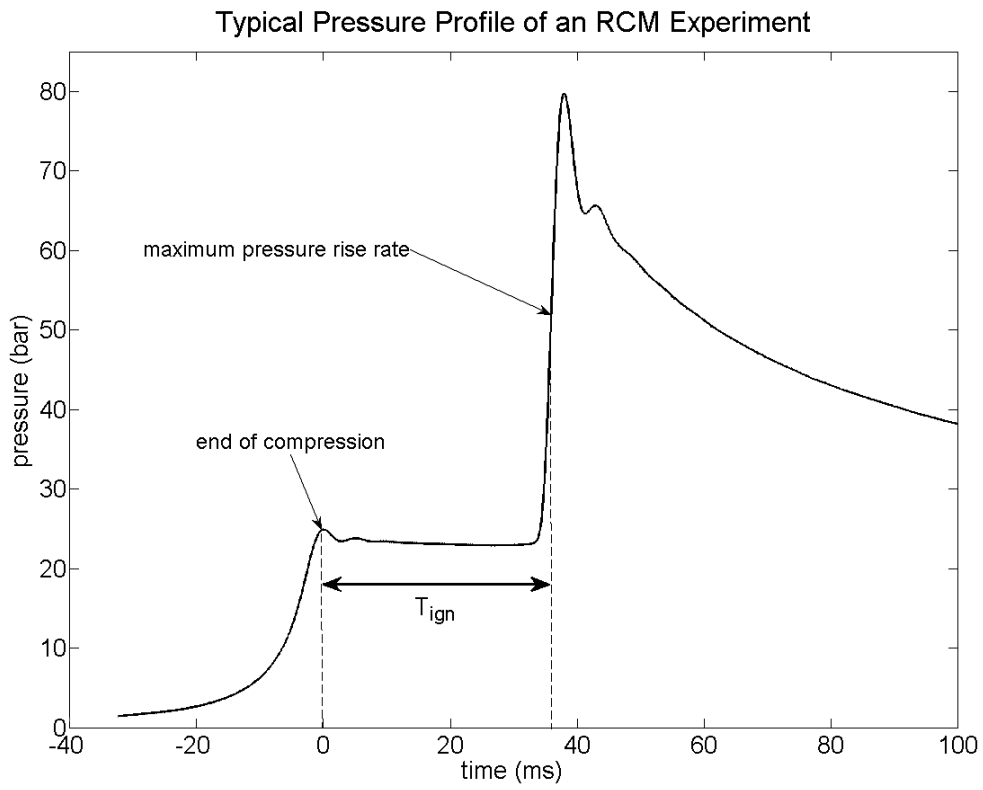


Fig. 3.4 Typical pressure profile of an RCM experiment

4. Results and Discussion

Ignition delays of isooctane-ethanol blend fuel are measured under various conditions and results are plotted over a post-compression temperature ranging from 800 to 880 K. Measured ignition delays show different characteristics upon the temperature range. Tested results are analyzed under two different regions, 800 - 840 K and 850 - 880 K. Fuel-air mixture occasionally fails to self-ignite below 800 K because of temperature decline where continuous heat loss to the combustion chamber wall occurs during relatively longer ignition delay period.

4.1 Experimental Results

Under 800 - 840 K region, ignition delay of fuel-air mixture increases remarkably with higher ethanol content. In Fig. 4.1, it is clearly noticeable that the gap between the ignition delays of E0 (pure isooctane) and E100 (pure ethanol) is almost an order of magnitude. Generally, ignition delay of mixture increases with higher ethanol content which represents the higher ON of ethanol compared to isooctane. Nevertheless, ignition delay characteristics of blends are similar when ethanol content is higher than 50 %. This trend is also observed in studies of Kasseris et al. [6] where they have mentioned that “chemical” effect of ethanol in increasing ON is

limited to a certain extent when there is 50% or more ethanol in isooctane-ethanol blend fuel.

There is an interesting trend for the pure isooctane case which shows almost “flat” curve under the low temperature region, meaning that temperature does not affect the reactivity of mixture. This curve could even be transformed to the region in which ignition delay gets shorter with decreasing temperature. That is not a normal case of chemical reactivity. Some hydrocarbons such as isooctane go through specific reaction pathways under 700 - 800 K region and may need shorter time for self-ignition compared to relatively higher temperature domain. This trend is named “negative temperature coefficient (NTC)” and it is reported and investigated by multiple researchers. [9, 16]

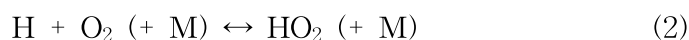
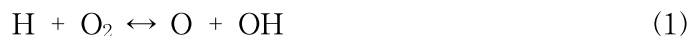
Under 850 - 880 K domain, the merit of ethanol as a ignition delay extender diminishes. In Fig 4.1 gap of ignition delay between ethanol-containing blends disappears at approximately 850 K and thereafter. In E100 case, reactivity of fuel-air mixture seems stimulated at higher temperatures where overall reaction and combustion of fuel-air mixture is almost same or even faster than E0. In addition, reaction characteristics of ethanol seems very sensitive to temperatures above 850 K, as experimental results are scattered in that region.

4.2 Chemical Kinetics Modeling Analysis

4.2.1 800 - 840 K region

Different ignition characteristics of each blend are consequences of different reaction pathways. With small amount of ethanol included in isooctane, reaction pathway of isooctane is considerably affected.

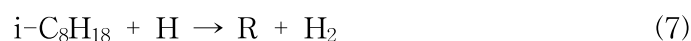
First of all, combustion radicals such as H, HO₂, H₂O₂, and OH must be continuously supplied for consecutive reaction and combustion of fuel molecules. These species are formed in following reaction pathways of hydrogen-oxygen kinetics such as,



and miscellaneous reactions thereafter. M denotes third body species which do not participate in reactions with other molecules but affect the speed or efficiency of a specific reaction.

Along with H₂-O₂ kinetics, hydrogen atom is detached from an isooctane

molecule with the participation of combustion radicals under this temperature region. Four distinct alkyl radicals (isooctyl radicals, prefixes α , β , γ , and δ) can be formed via H abstraction from different sites of the molecule. An alkyl radical is generally referred to as R when describing the reaction process,



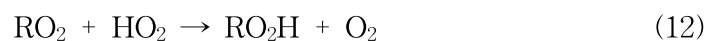
They are added to molecular oxygen and form alkylperoxy radicals as,



Propagation process continues with reactions of alkyl radicals with alkylperoxy radicals as,



or reactions with other species,

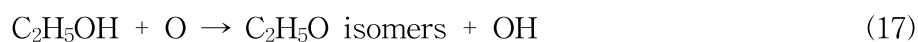


Also, an isomerization of alkylperoxy radical rearranges the atoms,



and following reactions of QOOH to cyclic ethers, olefins, or other species are major pathway of isooctane oxidation. [10] Here Q denotes olefins (C_nH_{2n}).

Existence of ethanol in blend fuel drastically alters the initial process of isooctane oxidation. Ethanol kinetics are investigated and continuously updated by Marinov [17], Li et al. [12], Hass et al. [18], and other researchers. Initiation processes between an ethanol molecule and combustion radicals are presented as,



and their reaction rate coefficients are continuously updated. Reactions (15) - (19) tell us that ethanol molecules also “consume” the combustion radicals at the first step of H abstraction reactions and their radical species propagate through their own reaction pathway. Therefore, decrease in concentration of the combustion radicals slows down both the radical chain reactions (1) - (6) and alkyl formation processes of (7) - (9), leading to longer ignition delay of ethanol-isooctane blend fuels for sufficient radical formation and combustion.

Due to lack of reactions (15) - (19) included in the isooctane model, we couldn't compare the reaction rates of (7) - (9) and (15) - (19) directly. Instead, reaction rate of (7) is investigated for evaluation of the H

consumption by ethanol pathway as it is thought that decrease in concentration of H would slow down the initial H abstraction from molecular isooctane. Figure 4.2 shows considerable difference with various isooctane-ethanol blends that speed of reaction (7) goes slower as ethanol content goes higher, leading to overall longer ignition delay necessary for combustive radical formation.

Figures 4.3 - 4.10 are alkyl radical species mass versus time plots derived by computational chemical kinetics using LLNL full isooctane model. There is no significant difference in radical species formation between E50 and higher fuels, thus plots are only given for E0, E10, E20, and E50 cases. Initial formation trends of alkyl radicals for pure isooctane and ethanol-containing fuels show considerable differences during the first few milliseconds, in detail sudden increase of alkyl radicals at around 5 ms only appears in E0 case. As an alkyl is formed, immediate addition of molecular oxygen occurs and appearance of massive RO_2 is observed. Compared to this, H abstraction reactions of isooctane are suppressed when ethanol consumes H, thereby alkyl formation process is rather smooth.

4.2.2 850 - 880 K region

Reaction pathway of isooctane under this temperature region is similar as

that of 800 - 840 K region. Thorough studies of isooctane reaction mechanism mention that the predominant H abstraction processes and alkyl radical reactions below 900 K are (7) - (10), which are same as that of 800 - 840 K case. With this in mind, it seems quite reasonable that transition of ignition delay trends is mainly affected by the ethanol reaction pathway.

Thermal decomposition of molecular ethanol is activated and dissociation into several intermediates occurs as follows,

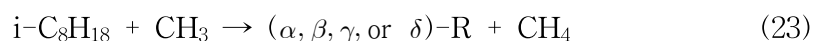


In these reactions, highly unstable species such as methyl radical (CH_3) is formed and this stimulates overall ethanol reactions by continuously breaking up molecular ethanol through H abstraction. For example, reaction rates of (20) of E100 fuel for temperatures of 860, 900, and 950 K are plotted in Figs. 4.11 and 4.12 for comparison of methyl radical formation extent.

Alkyl formation trends of various blends are shown in Figs. 4.13 - 4.16. Unlike the case of 800 - 840 K kinetics, alkyl radicals appear in similar trend from the initial moment regardless of ethanol percentage. Along with alkyl formation, next steps of reaction pathway such as addition to

molecular oxygen, RO₂ isomerization, and other principal kinetics are also similar in every blend.

Reaction rates of four distinct alkyl formation steps with CH₃ addition,



under 800 - 840 K and 850 - 880 K region show considerable differences. For example, reaction rates of (23) for E10 fuel under two different temperature conditions are shown in Fig. 4.17. In 860 K case, vigorous reactions between molecular isooctane and methyl radical from ethanol molecule are observed while in 800 K reaction (23) seems to have no significant effect during the initiation stage.

4.3 Limitations and Future Works

4.3.1 Imperfection in the chemical kinetic models

Unfortunately, there are several limitations on accurate analysis of ignition delay for isooctane-ethanol blend fuel. Reactions (15) - (19) are thought to play a major role in 800 - 840 K region, but only limited number of reactions involving ethanol are included in the isooctane model. Therefore, precise estimation of ethanol-originated species such as C₂H₄OH isomers are not feasible. For reaction (19) Lee et al. [19] mentioned that this reaction has so far not been theoretically or experimentally studied but

only estimated rate constants are reported. In addition, reactions (20) - (22) are also excluded in the isooctane model, thus only restricted approach for the thermal decomposition pathway of molecular ethanol could be possible. Lack of these reactions may be the cause of inaccurate estimation of ignition delays by computational approach, especially for the isooctane-ethanol blends. In Fig 4.18, experimental and computational results are compared where accuracy of the isooctane kinetics model is poor for ethanol-blended cases.

Princeton's updated ethanol model shows good reproducibility of the experimental results under 800 - 840 K, but in case of higher temperature conditions additional modification of the model and alterations to the reaction coefficients might be helpful. For example, in Fig. 4.12 methyl radical formation rates are compared for various temperature cases, where the model assumes a lower limit of 900 K for considerable thermal decomposition process of molecular ethanol. Our experimental results argue that this lower limit can be extended further to 860 K.

4.3.2 Future works

Although lots of studies were performed for the chemical kinetics of pure isooctane or pure ethanol, there are almost no considerations for the blend fuels of the two substances. This gives a strong motivation to us and

our next work will be focused on the combination of the isooctane and ethanol model and evaluation of the merged mechanism. Alterations to the experimental apparatus for optical accessibility would further help us measure the radicals during the test process, which gives a strong basis in supporting our arguments.

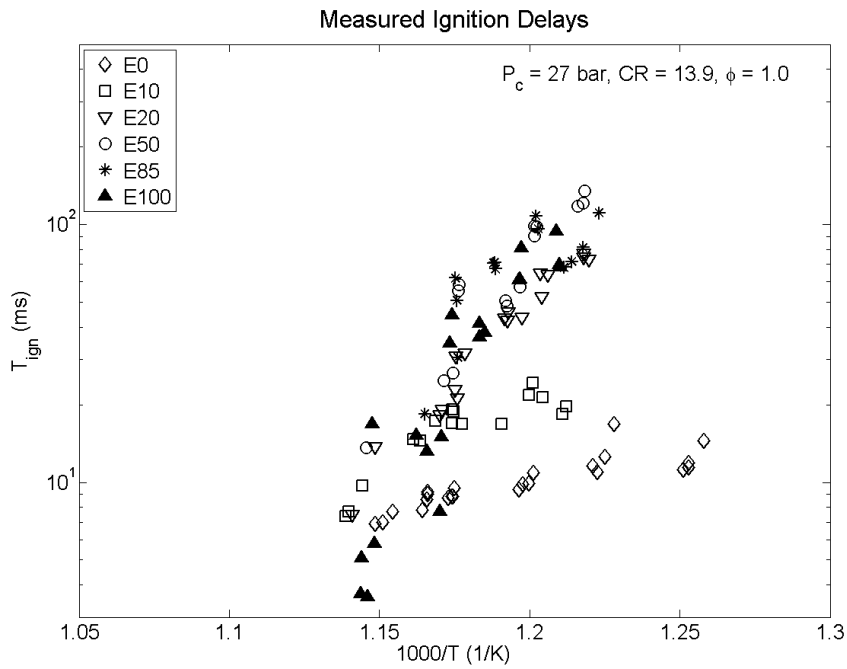


Fig. 4.1 Measured ignition delays of blends

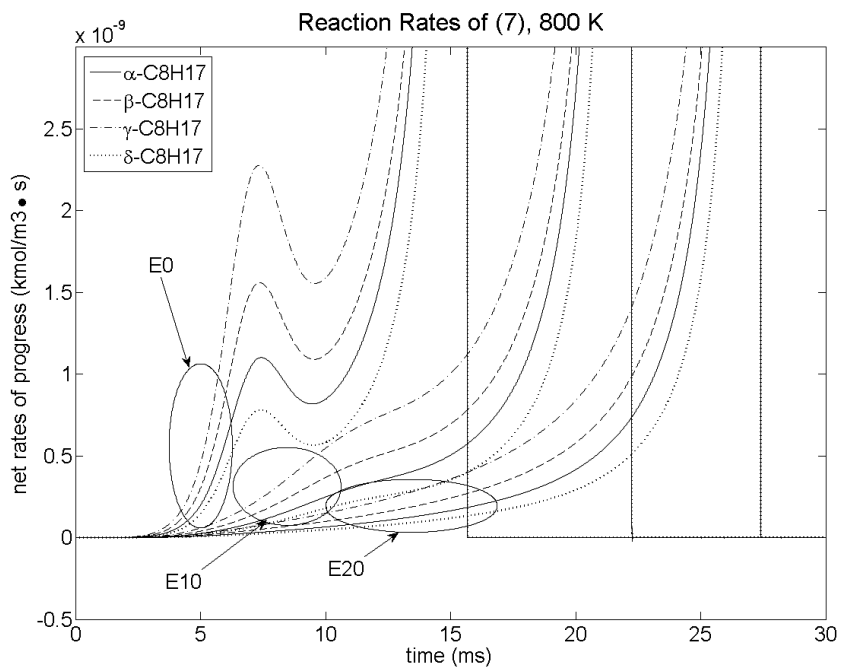


Fig. 4.2 Reaction rates of $i\text{-C}_8\text{H}_{18} + \text{H} \rightarrow \text{R} + \text{H}_2$

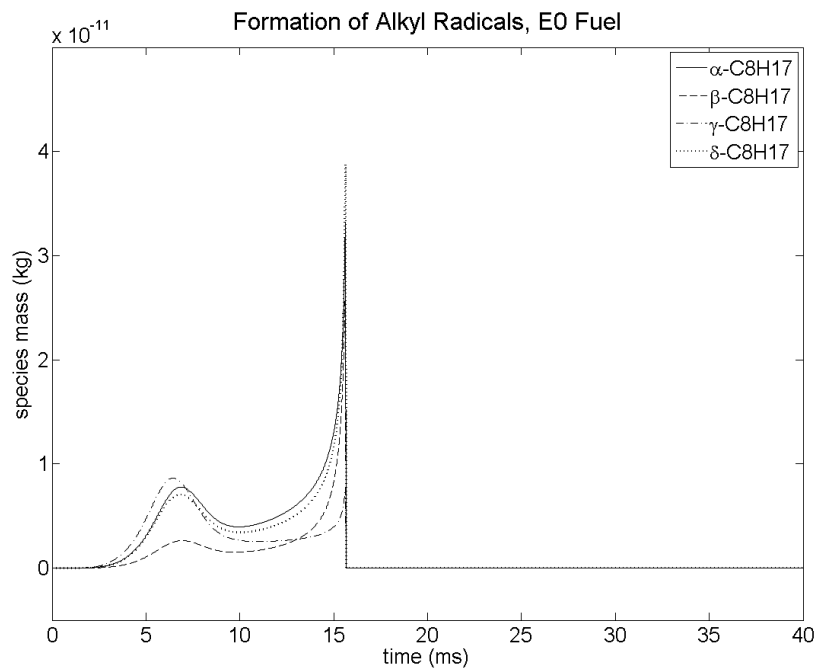


Fig. 4.3 Alkyl radical mass versus time at 800 K, E0

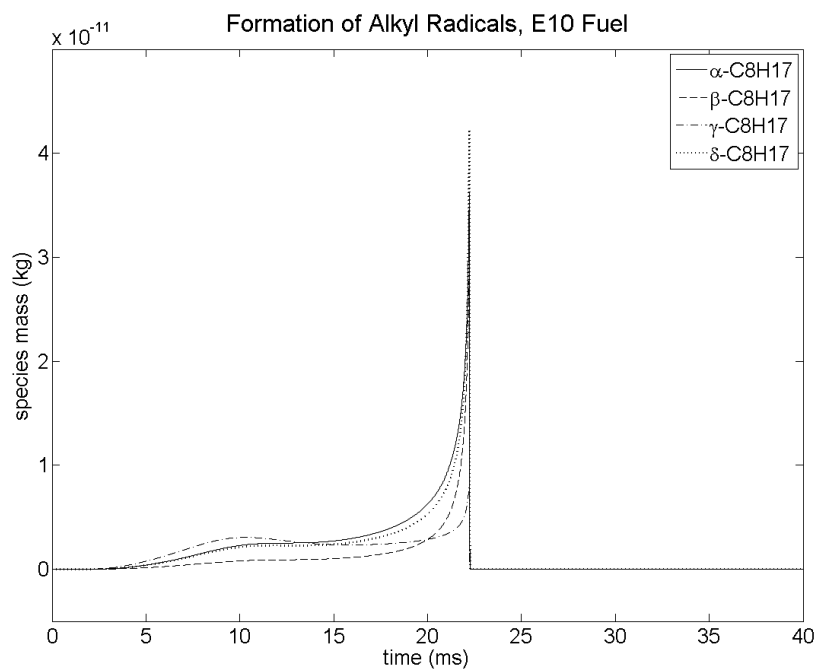


Fig. 4.4 Alkyl radical mass versus time at 800 K, E10

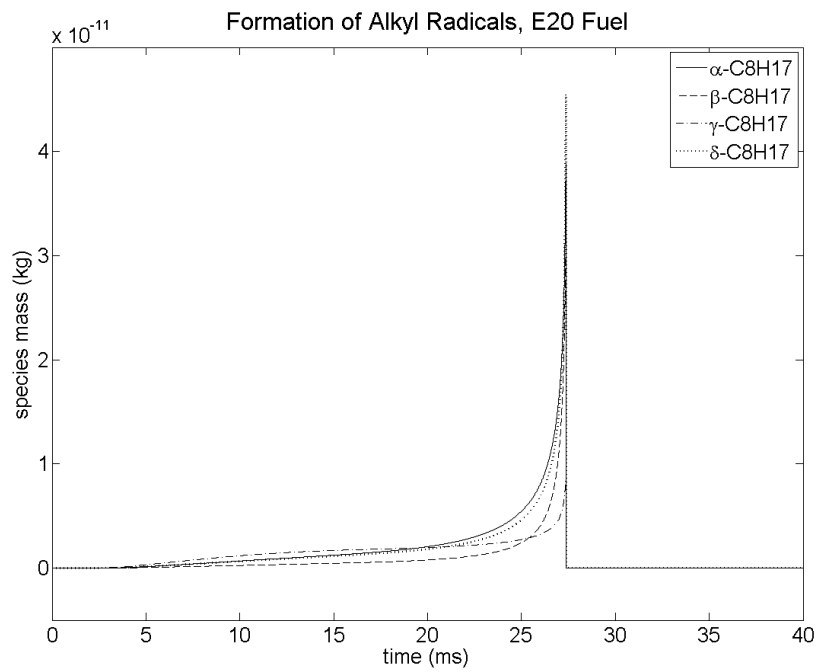


Fig. 4.5 Alkyl radical mass versus time at 800 K, E20

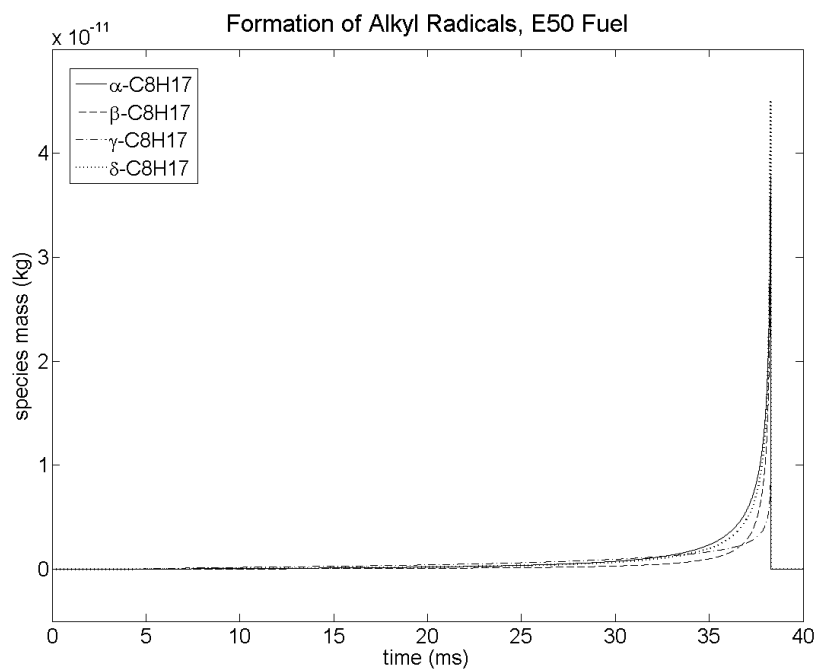


Fig. 4.6 Alkyl radical mass versus time at 800 K, E50

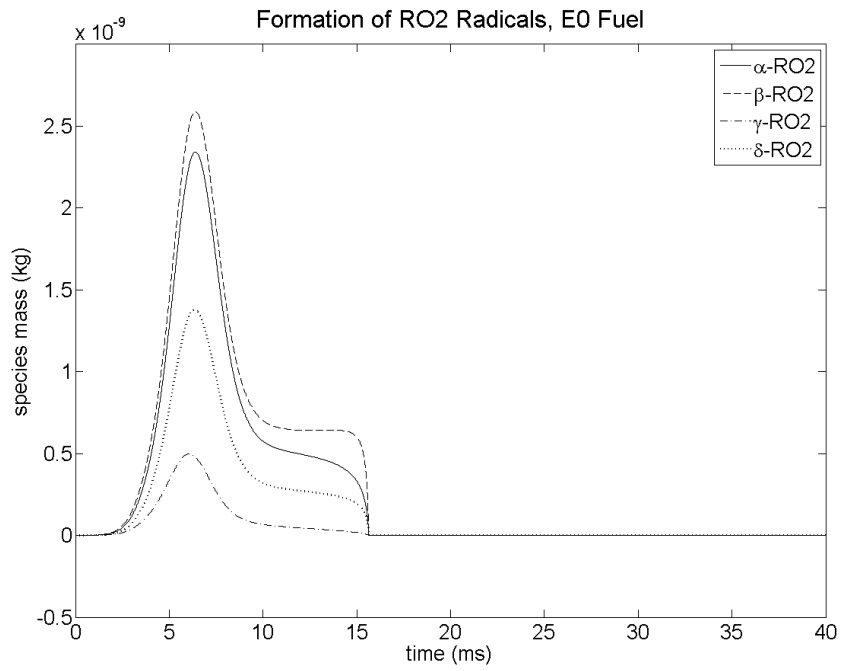


Fig. 4.7 RO₂ radical mass versus time at 800 K, E0

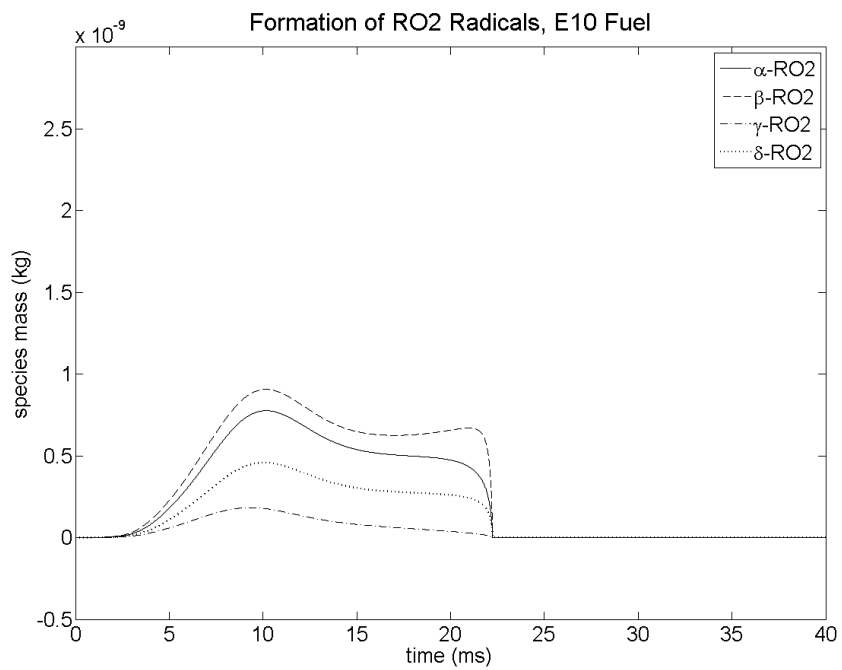


Fig. 4.8 RO₂ radical mass versus time at 800 K, E10

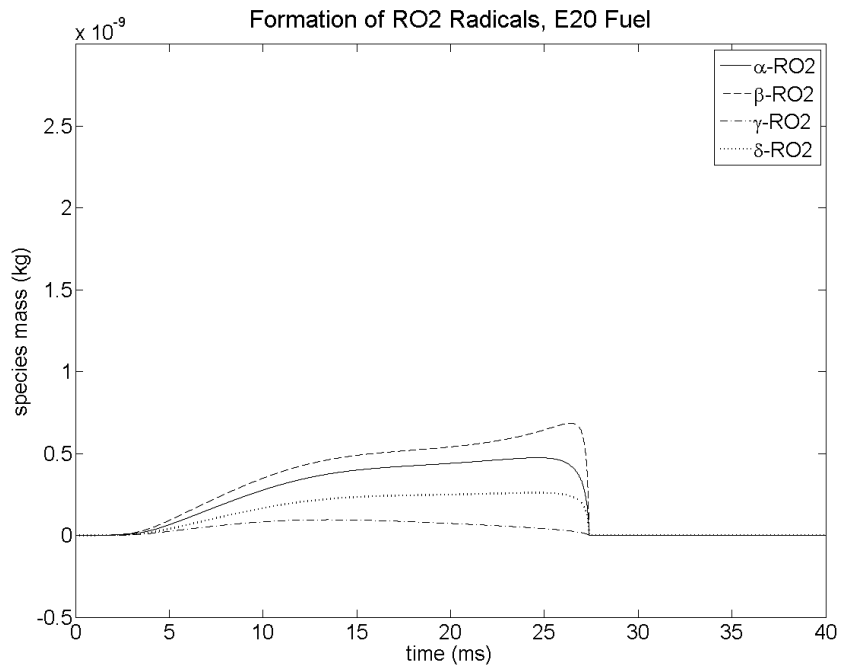


Fig.4.9 RO₂ radical mass versus time at 800 K, E20

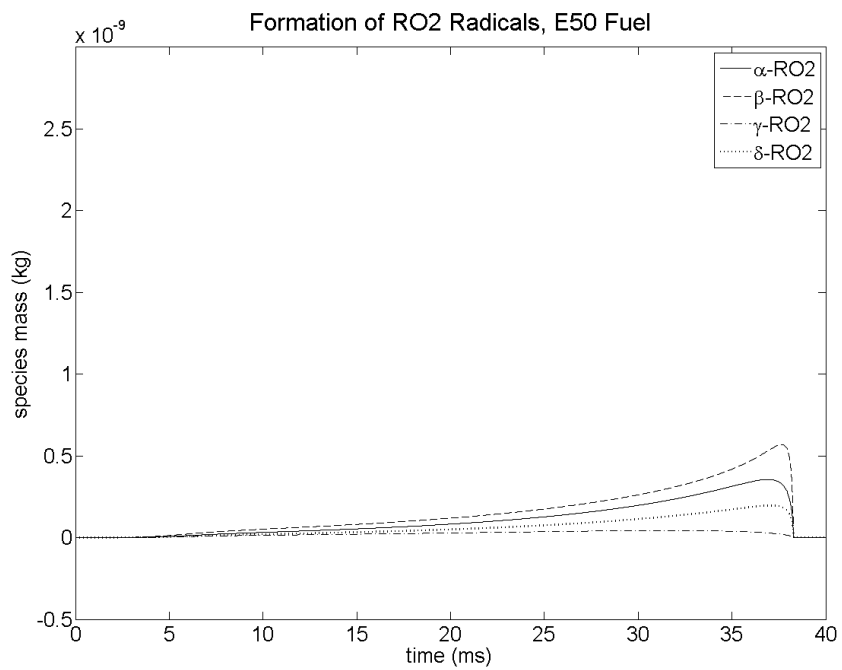


Fig. 4.10 RO₂ radical mass versus time at 800 K, E50

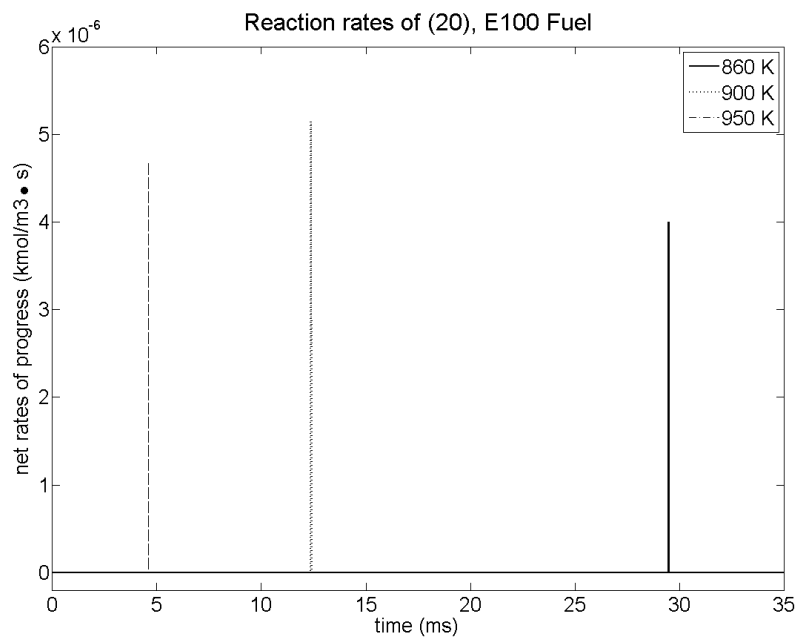


Fig. 4.11 Reaction rates of $C_2H_5OH (+ M) \rightarrow CH_2OH + CH_3 (+ M)$

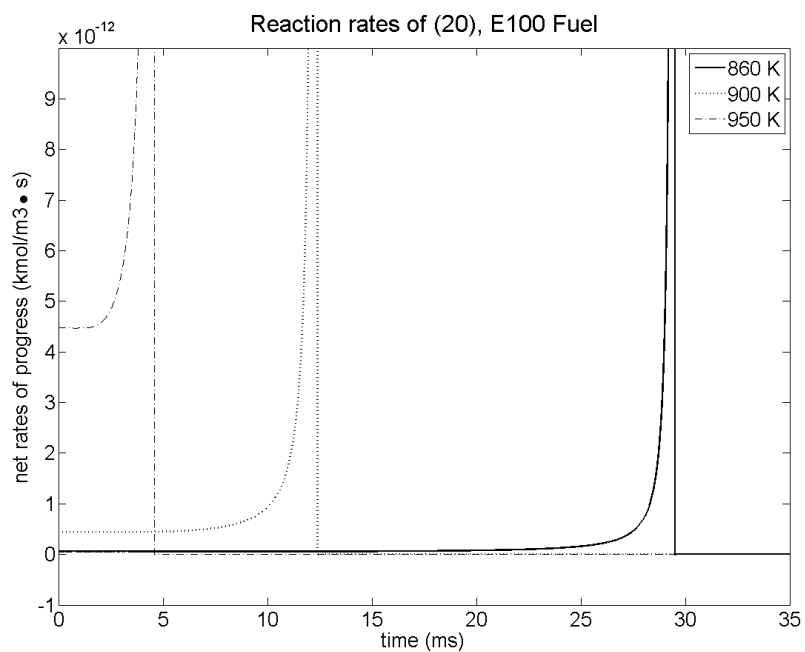


Fig. 4.12 Magnification of Fig. 4.11

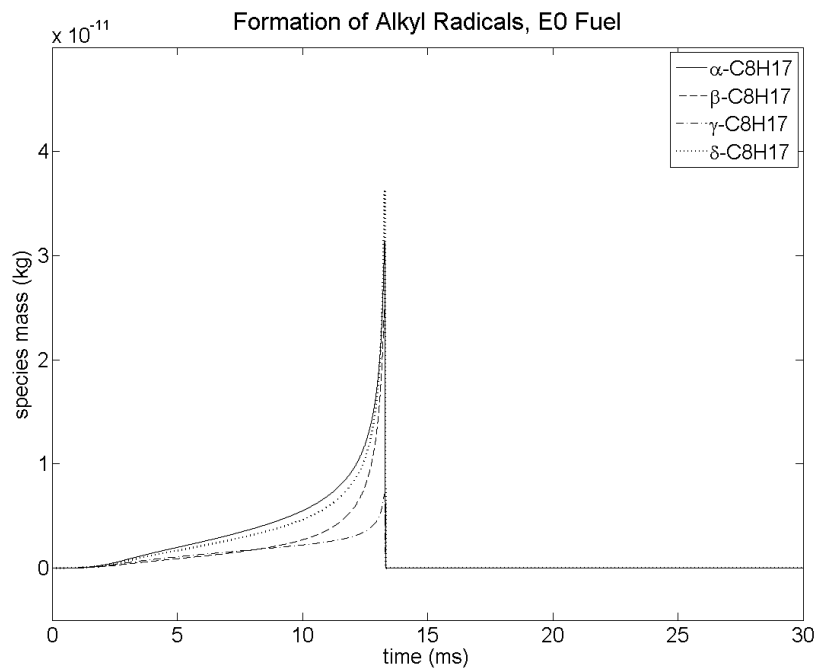


Fig. 4.13 Alkyl radical mass versus time at 860 K, E0

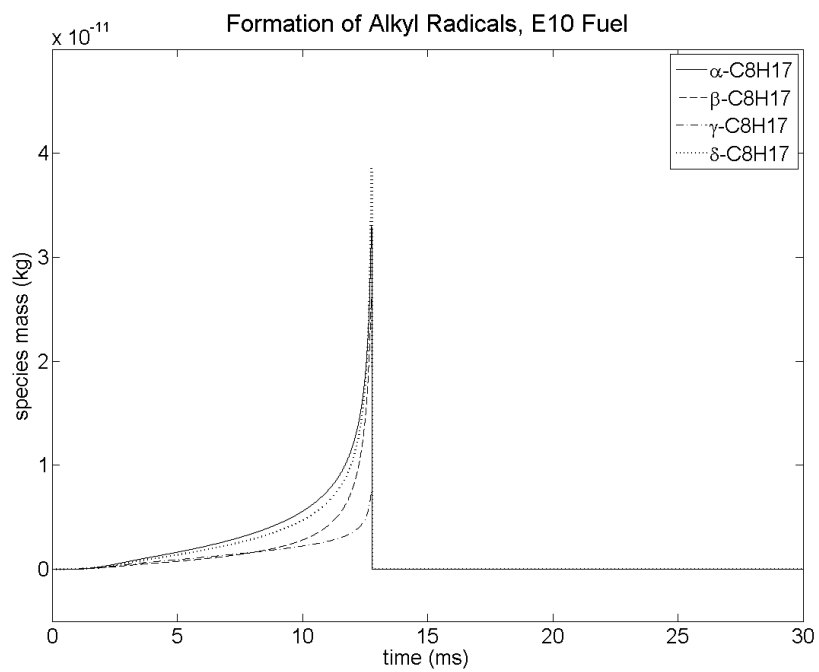


Fig. 4.14 Alkyl radical mass versus time at 860 K, E10

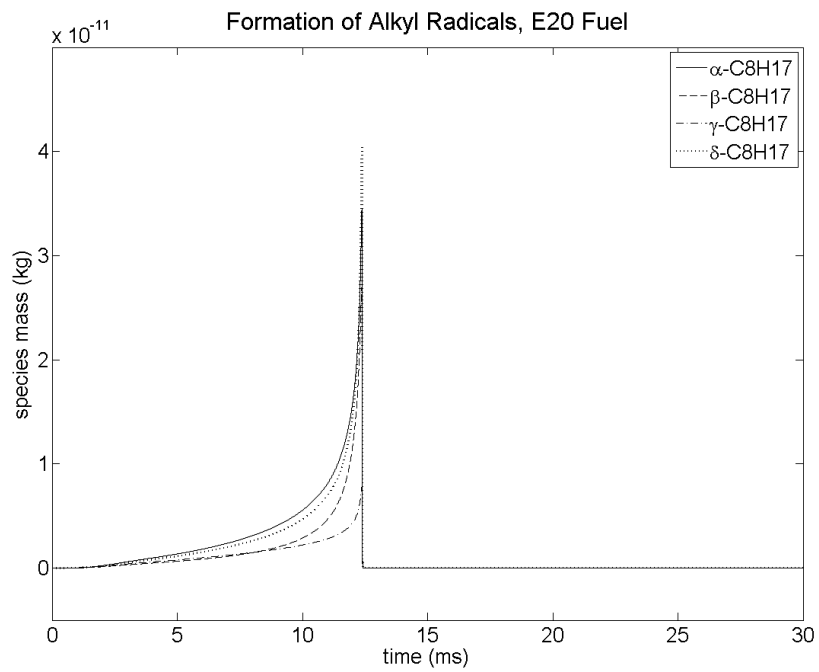


Fig. 4.15 Alkyl radical mass versus time at 860 K, E20

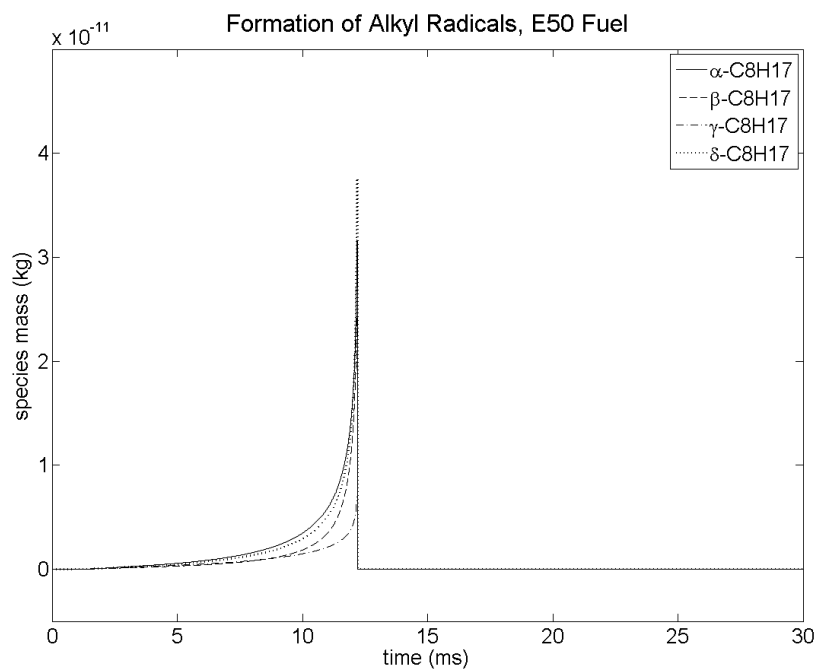


Fig. 4.16 Alkyl radical mass versus time at 860 K, E50

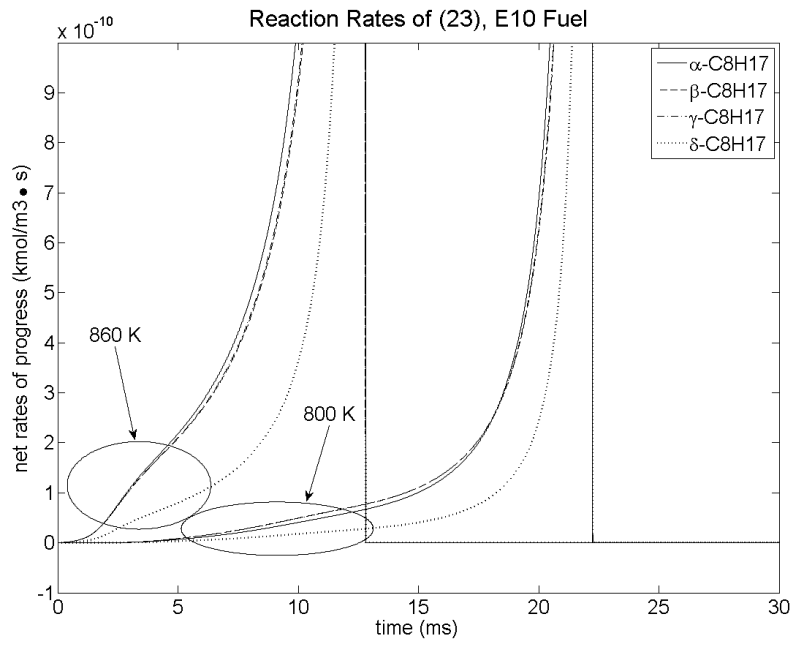


Fig. 4.17 Reaction rates of (23)

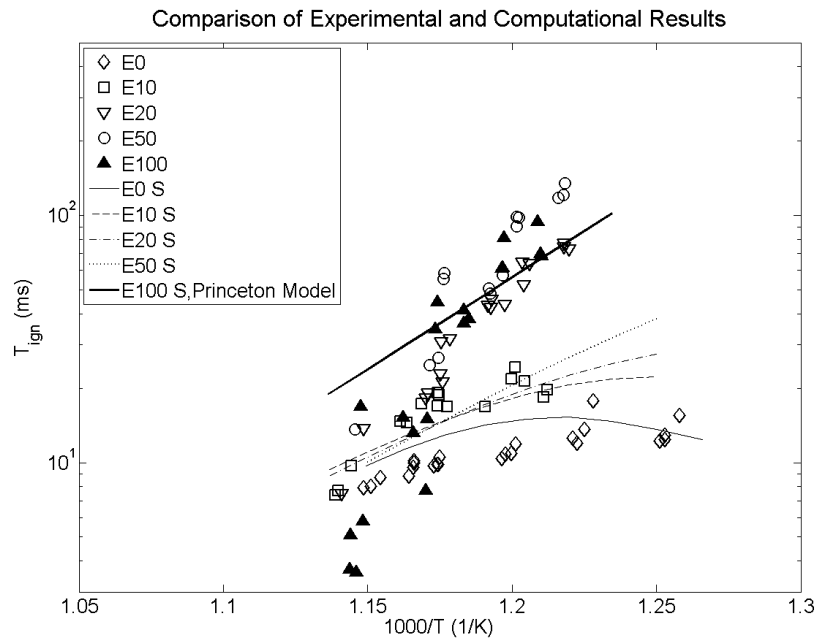


Fig. 4.18 Comparison of experimental and computational results

5. Conclusions

Fundamental studies are performed for understanding the knock characteristics of gasoline-ethanol blend fuel in SI engine. Isooctane is selected as a surrogate fuel of gasoline. Ignition delays of isooctane-ethanol blend fuel under various conditions are measured by using a rapid compression machine and experimental results are analyzed with the help of chemical kinetics modeling study. Results are as follows:

1. Experimental results show that ethanol plays a major role under 800 - 840 K temperature conditions. Ignition delay tends to be considerably longer with the addition of ethanol into isooctane, but there is no significant differences after ethanol content is 50 % (by volume) or higher. H consumption by molecular ethanol seems to be the primary reason for this phenomenon.
2. The characteristic of ethanol as a reaction-delaying agent diminishes as tests are performed under 850 - 880 K region in which ignition delays of various blends show little difference. Major reaction pathway of ethanol seems to be quite distinct from that of 800 - 840 K region.
3. Chemical kinetics models are broadly utilized as an effective tool for analyzing combustion of various substances. Both the isooctane mechanism and the ethanol mechanism show good agreement with the

experiment results when pure substances are tested, but in case of the blend fuel reproduction of experiment is limited to a certain extent.

4. Future works will be focused on mutual relationship between reaction pathways of isooctane and ethanol respectively.

References

1. Puerto Rico, J. A. “Programa de Biocombustíveis no Brasil e na Colômbia: uma análise da implantação, resultados e perspectivas” (in Portuguese), Ph.D. Dissertation, Universidade de São Paulo, 2008,
2. Heywood, J. B. *Internal Combustion Engine Fundamentals*. New York: McGraw-Hill, 1988.
3. Cancino, L. R., Fikri, M., Oliveira, A. A. M., and Schulz, C. “Ignition delay times of ethanol-containing multi-component gasoline surrogates: Shock-tube experiments and detailed modeling”, *Fuel*, Vol. 90, 2011, pp. 1238 - 1244.
4. Dagaut, P., and Togbé, C. “Oxidation Kinetics of Mixtures of Iso-octane with Ethanol or Butanol in a Jet-Stirred Reactor: Experimental and Modeling Study”, *Combustion Science and Technology*, Vol. 184, 2012, pp. 1025 - 1038.
5. Kasseris, E., and Heywood, J. “Charge Cooling Effects on Knock Limits in SI DI Engines Using Gasoline/Ethanol Blends: Part 1 - Quantifying Charge Cooling”, SAE paper 2012 - 01 - 1275, 2012.
6. Kasseris, E., and Heywood, J. “Charge Cooling Effects on Knock Limits in SI DI Engines Using Gasoline/Ethanol Blends: Part 2 - Effective Octane Numbers”, SAE paper 2012 - 01 - 1284, 2012.
7. Lumley, J. L. *Engines: An Introduction*. Cambridge University Press,

New York, 1999

8. Pulkrabek, W. W., *Engineering Fundamentals of the Internal Combustion Engine. 2nd ed*, Pearson Prentice - Hall, 2004
9. Mehl, M., Curran, H. J., Pitz, W. J., and Westbrook, C. K. "Chemical kinetic modeling of component mixtures relevant to gasoline", Proc. 4th European Combustion Meeting, 2009.
10. Curran, H. J., Gaffuri, P., Pitz, W. J., and Westbrook, C. K. "A Comprehensive Modeling Study of iso-Octane Oxidation", Combustion and Flame, Vol. 129, 2002, pp. 253 - 280.
11. Curran, H. J., Gaffuri, P., Pitz, W. J., and Westbrook, C. K. "A Comprehensive Modeling Study of n-Heptane Oxidation", Combustion and Flame, Vol. 114, 1998, pp. 149 - 177.
12. Li, J., Kazakov, A., Chaos, M., and Dryer, F. L. "Chemical Kinetics of Ethanol Oxidation", Proc. 5th US Combustion Meeting, 2007.
13. Kim, Y. "A Study on the CAI Combustion Characteristics Using a Reduced Chemical Kinetic Mechanism", Ph. D. Thesis, Seoul National University, 2007.
14. Schreiber, M., Sadat Sakak, A., Lingens, A., and Griffiths, J. F. "A Reduced Thermokinetic Model for the Autoignition of Fuels with Variable Octane Ratings", Proc. 25th Symposium on Combustion, 1994, pp. 933 - 940.
15. Tanaka, S., Ayala, F., Keck, J. C., and Heywood, J. B. "Two-stage

- ignition in HCCI combustion and HCCI control by fuels and additives”, *Combustion and Flame*, Vol. 132, 2003, pp. 219 - 239.
16. Goldsborough, S. S. “A chemical kinetically based ignition delay correlation for iso-octane covering a wide range of conditions including the NTC region”, *Combustion and Flame*, Vol. 156, 2009, pp. 1248 - 1262.
 17. Marinov, N. M. “A Detailed Chemical Kinetic Model for High Temperature Ethanol Oxidation”, *Int. Journal of Chemical Kinetics*, Vol. 31, 1999, pp. 183 - 220.
 18. Haas, F. M., Chaos, M., and Dryer, F. L. “Low and intermediate temperature oxidation of ethanol and ethanol-PRF blends: An experimental and modeling study”, *Combustion and Flame*, Vol 156, 2009, pp.2346 - 2350.
 19. Lee, C., Vranckx. S., Heufer, K. A., Khomik, S. V., Uygun. Y., Oliver. H., and Fernandes, R. X. “On The Chemical Kinetics of Ethanol Oxidation: Shock Tube, Rapid Compression Machine and Detailed Modeling Study”, *Zeitschrift für Physikalische Chemie*, Vol. 226, 2012, pp.1 - 27.

요약

불꽃점화 엔진에서 노킹 방지를 위한 이소옥탄-에탄올 혼합 연료의 점화지연 특성에 관한 실험적 연구

서울대학교 대학원
기계항공공학부
송화섭

다운사이징과 온실가스 배출저감은 21세기 자동차업계의 가장 큰 관심사들 가운데 하나이다. 이를 위해서 노킹과 같은 기술적 문제에 대한 해결이 필요하다. 이에 관련하여 일반적으로 노킹을 방지하는데 도움이 된다고 알려진 에탄올을 가솔린의 모사연료인 이소옥탄과 혼합하여 급속압축장치(RCM)를 이용하여 여러 가지 조건에서의 점화지연을 측정하였다. 또한 실험결과를 분석을 위해 화학 반응 모델을 이용하였다. 연구 결과 800 - 840K 의 온도 영역에서는 에탄올의 포함 여부가 점화지연을 길어지게 하는 주요 원인으로 밝혀졌다. 반면에 850 - 880K 의 온도 영역에서는 에탄올의 존재가 큰 변화를 나타내지 않았다. 또한 두 경우 모두 혼합 연료 중 에탄올의 함량이 50% 이상인 경우 비슷한 경향을 나타냈다. 실험 결과를 분석해 보면, 에탄올의 초기 화학 반응이 어떻게 진행되느냐에 따라 전체적인 혼합 연료의 점화 지연 경향이 결정된다는 것을 알 수 있다. 그러나 화학 반응 모델의 불완전성을 받

견할 수 있었으며, 이에 대한 추가적인 개선을 통해 실험 결과를 더 잘 재현할 수 있을 것으로 기대된다.

주요어: 점화지연, 노킹, 급속압축장치, 화학 반응 모델, 이소옥탄-에탄올 혼합 연료

학번: 2011-20716